

## Characterization of Synthesized $\text{NiCo}_2\text{O}_4$ with Trisodium Citrate for Supercapacitor Material: A Preliminary Study

Andriono Manalu<sup>1\*</sup>, Istas Pratomo Manalu<sup>2</sup>, Muktar Bahruddin Panjaitan<sup>1</sup>, Ady Frenly Simanullang<sup>1</sup>, Parlindungan Sitorus<sup>3</sup>

<sup>1</sup>Department of Physics Education, Faculty of Teacher Training and Education, Universitas HKBP Nommensen Pematangsiantar, Pematangsiantar, 21132, Indonesia

<sup>2</sup>Department of Computer Engineering, Vocational Faculty, Del Institute of Technology, Toba, 22381, Indonesia

<sup>3</sup>Department of Physics Education, Faculty of Teacher Training and Education, Universitas HKBP Nommensen, Medan, 20155, Indonesia

\*Corresponding author: andriono.manalu@uhnp.ac.id

### Abstract

Supercapacitors can be called electrostatic double-layer capacitors (EDLCs) or pseudo-capacitors based on their energy storage mechanism. Pseudo-capacitors with metal oxide electrodes that transmit electric charge offer great application power but low stability. This study aims to characterize trisodium citrate (TSC) modified  $\text{NiCo}_2\text{O}_4/\text{rGO}$  electrodes as a preliminary study for the  $\text{NiCo}_2\text{O}_4$  nanoparticle pseudo-capacitor. The materials were characterized using SEM (Scanning Electron Microscopy), XRD (X-Ray Diffractometer), FT-Raman (Fourier Transform Raman Spectroscopy), and FTIR (Fourier Transform Infrared Spectroscopy). All of these analyses confirmed that  $\text{NiCo}_2\text{O}_4$  was manufactured successfully using TSC. At XRD, the angles of  $2\theta$ , namely  $45.04^\circ$  and  $53.34^\circ$ , matched the plane of the cubic phase nanorod crystals of  $\text{NiCo}_2\text{O}_4$  with values of 400 and 511, respectively. In the Raman examination, the presence of rGO, which increased the crystallinity of  $\text{NiCo}_2\text{O}_4$  nanoparticles, was confirmed. FTIR analysis indicated that the  $1550\text{--}1600\text{ cm}^{-1}$  corresponds to a C=C functional group in an aromatic ring or a C=O  $\pi\text{--}\pi$  structure, and the wavenumber of  $2300\text{ cm}^{-1}$  corresponds to the OH group in TSC, an alkanoate derivative. SEM analysis determined that  $\text{NiCo}_2\text{O}_4$  nanoparticles with 1 mmol TSC are the ideal material for supercapacitor electrodes, as the structure is the most uniform, soft, and tidy. Further analysis is needed to confirm the stability of the modified material.

### Keywords

$\text{NiCo}_2\text{O}_4$ , rGO, Trisodium Citrate, Supercapacitor, Pseudo-capacitor

Received: 9 December 2022, Accepted: 5 March 2023

<https://doi.org/10.26554/sti.2023.8.2.245-251>

## 1. INTRODUCTION

In this modern age, the advancement of knowledge in technology has a significant impact on human existence. The increasing population and a more wasteful lifestyle have led to an increase in energy demand. To satisfy this demand, enormous quantities of fuel must be supplied at a premium price. Due to insufficient storage technology, a significant amount of generated energy is wasted. Current energy storage methods are prohibitively expensive or environmentally hazardous in numerous ways (Mehta et al., 2020). Therefore, more research and development efforts are required to identify renewable energy sources that are efficient, cost-effective, and environmentally friendly (Bhat et al., 2023). One is the invention of a device for storing and utilizing energy. Several advancements in energy storage and conversion technology, such as solar cells, fuel cells, compressed hydrogen, supercapacitors, and batteries, have been made over the past two decades to use sustainable energy storage and conversion systems professionally (Ren and

Huang, 2022).

Based on their environmental and economic benefits, the device components (electrodes and electrolytes) should ideally be accessible in a straightforward, economical, and environmentally friendly manner with the appropriate final characteristics (Mehta et al., 2020). The primary requirement for electrical energy derived from renewable resources is an efficient energy storage system (ESS). Batteries and supercapacitors are the most in-demand forms of energy storage in the current digital era (Zheng et al., 2023). A supercapacitor or electrochemical capacitor is an electric double layer that serves as an energy storage device based on the charging and discharging of the dielectric interface electrode (Wang et al., 2015). Supercapacitors offer a high-power density, the capacity to charge quickly, store 10–100 times more energy than batteries, and long service life (>100,000 cycles) (Simon and Gogotsi, 2020). Based on their energy storage technique, supercapacitors can be called electrostatic double-layer capacitors (EDLCs) or pseudo-capacitors (Winter and Brodd, 2004). EDLC capacitors are typically

utilized in low-power applications (Karthikeyan et al., 2021), using activated carbon electrodes that have a wide surface area to store electric charges at the electrode/electrolyte interface, such as carbon fiber, carbon aerogel, graphene, and carbon nanotubes (Jiang et al., 2018). The capacitor's power density and stability are excellent, but its specific capacitance is poor (Faraji and Ani, 2015).

With metal oxide electrodes whose electric charge transfer is based on reversible Faradaic processes (Najib and Erdem, 2019), including redox processes on metal oxides, reversible adsorption, and reversible electrochemical doping on conductive polymers for electrodes, pseudo capacitors have a high application power (Abdah et al., 2020). These capacitors generally have a greater energy density and specific capacitance than EDLCs but lower stability (Manalu et al., 2022; Shi et al., 2011). In order to improve the performance of the pseudo-capacitor, more research is required.

Transition metal oxides, such as RuO<sub>2</sub>, MnO<sub>2</sub>, Co<sub>3</sub>O<sub>4</sub>, and NiO, are regarded as the most promising candidate for pseudo-capacitors due to their capacitance, which is many times that of carbon materials (Karimi et al., 2022). Using Ni and Co ions, NiCo<sub>2</sub>O<sub>4</sub> can currently be utilized as a supercapacitor electrode with extremely high performance. Additionally, these electrodes are abundant in nature, eco-friendly, and possess low toxicity (Km et al., 2022). According to Liu et al. (2021), nickel and cobalt-based oxide/hydroxide composites are commonly employed as electrode precursors as a potential cost-effective substitute for RuO<sub>2</sub>. In recent years, NiCo<sub>2</sub>O<sub>4</sub> has gained significant interest as an electrode material for high-performance supercapacitors, as it has been developed to be optimal for this purpose. Furthermore, according to various earlier investigations, NiCo<sub>2</sub>O<sub>4</sub> has superior electrical conductivity over NiO and Co<sub>3</sub>O<sub>4</sub> (Lee et al., 2019).

Many studies have been conducted on transition metal oxides, binary transition metal oxides, and their combination with rGO for producing energy storage device materials (Wang et al., 2015). Graphene is an exciting form of carbon due to its high volume-to-surface ratio and high conductivity. It possesses important qualities for achieving high energy storage capacities and power densities in supercapacitors. As a material for energy storage, graphene's flexibility and electrochemical properties have been intensively investigated (Nakhodchari et al., 2023). Metal-based rGO nanocomposites have effectively exhibited multiple applications, such as sodium-ion batteries, hybrid supercapacitors, wastewater treatment, and photocatalytic properties. rGO also supports rapid faradic oxidation-reduction processes at the electrode surface, which adds to a high energy density relative to carbon-based materials and a significant charge storage (Saikia et al., 2020).

To maximize the performance of NiCo<sub>2</sub>O<sub>4</sub> supercapacitors, additional work is required to improve their stability. Diverse nanostructures can be fabricated using hydrothermal, chemical immersion deposition, adsorption, and ion coating reactions. These synthesis techniques can control the shape and size of nanoparticles. During the synthesis process, organic capping

agents such as polyethylene-glycol (PEG), polyvinylpyrrolidone (PVP), and trisodium citrate (TSC) alter the shape of nanomaterials (Dong et al., 2011). Trisodium citrate has been used extensively as a form guide in fabricating several metal oxide nanostructures (Han et al., 2013). Xing et al. (2012) manufactured mesoporous -Ni(OH)<sub>2</sub> and NiO nanospheres using ammonia and citrate using a hydrothermal method heated at 100 °C for 24 hours; the nanospheres exhibited a specific capacitance of 290 F g<sup>-1</sup>. With the addition of trisodium citrate to hierarchical NiO nanospheres, Han et al. (2013) discovered that the supercapacitor has a very high performance with a specific capacitance of 463 F g<sup>-1</sup> at 4.5 A g<sup>-1</sup> (90% capacity). In contrast, NiO without trisodium citrate only has a specific capacitance of 182 F g<sup>-1</sup> at 4.5 A g<sup>-1</sup>.

This study applied trisodium citrate to NiCo<sub>2</sub>O<sub>4</sub> nanomaterial electrodes as supercapacitor material. Therefore, this study aims to characterize the modified material for further use as a supercapacitor material. Characterization tests conducted with various instruments determined the morphological structure and the successful synthesis of NiCo<sub>2</sub>O<sub>4</sub> with trisodium citrate. As a preliminary study, this current study does not provide a test for supercapacitor application as the relevant study must be separated since it needs comprehensive related tests.

## 2. EXPERIMENTAL SECTION

### 2.1 Materials and Instrumental

The materials used were nickel(II) nitrate hexahydrate (Ni(NO<sub>3</sub>)<sub>2</sub>·6H<sub>2</sub>O), cobalt(II) nitrate hexahydrate (Co(NO<sub>3</sub>)<sub>2</sub>·6H<sub>2</sub>O), ammonium fluoride (NH<sub>4</sub>F), trisodium citrate (Na<sub>3</sub>C<sub>6</sub>H<sub>5</sub>O<sub>7</sub>), concentrated sulfuric acid (H<sub>2</sub>SO<sub>4</sub>), phosphoric acid (H<sub>3</sub>PO<sub>4</sub>), graphite powder, potassium manganate (KMnO<sub>4</sub>), hydrogen peroxide (H<sub>2</sub>O<sub>2</sub>), ammonium hydroxide (NH<sub>4</sub>OH), sodium hydroxide (NaOH), and ethanol (C<sub>2</sub>H<sub>5</sub>OH). These materials were obtained from Merck, Germany. Meanwhile, the instruments used for the characterization of the NiCo<sub>2</sub>O<sub>4</sub> sample with trisodium citrate (TSC) were SEM (Scanning Electron Microscope, FEI Quanta 650 FEG), X-Ray Diffraction (XRD, Philips XRD X'Pert MS), Fourier Transform Raman Spectroscopy (FT-Raman, RAMAN iHR320 HORIBA), and Fourier Transform Infrared Spectroscopy (FTIR, 8201 PC Shimadzu).

### 2.2 Methods

#### 2.2.1 Synthesis of NiCo<sub>2</sub>O<sub>4</sub> with TSC

The manufacture of NiCo<sub>2</sub>O<sub>4</sub> with trisodium citrate (TSC) adheres to the method developed by Paliwal and Meher (2020). With steady stirring, 35 mL of dilute Ni(NO<sub>3</sub>)<sub>2</sub>·6H<sub>2</sub>O (2 mmol) solution was mixed with 55 mL of dilute Co(NO<sub>3</sub>)<sub>2</sub>·6H<sub>2</sub>O (6 mmol) solution. A 50 mL aqueous solution of NH<sub>4</sub>F (16 mmol) and varying amounts of TSC (0.5, 1, and 2 mmol) were sequentially added to the mixture (see Table 1). Using an aqueous NaOH solution (1.0 M), the pH of the resultant solution was raised to 11. The solution was heated at 160°C (5°C min<sup>-1</sup>) for 24 hours in an autoclave coated with teflon and stainless steel. The product in the autoclave was cooled to

ambient temperature, and the precipitate formed was washed sequentially with water, a combination of water and ethanol, and 100% ethanol using a 5000 rpm centrifuge. The product was subsequently dried at 60°C in a vacuum oven, and the resulting product was treated to a 3-hour heat treatment at 350°C (using a heating path of 5°C min<sup>-1</sup>) under an ambient atmosphere. A black powder product identified as NiCo<sub>2</sub>O<sub>4</sub> with TSC was obtained. NiCo<sub>2</sub>O<sub>4</sub> without TSC, also known as NiCo<sub>2</sub>O<sub>4</sub> pristine, was used for comparison.

### 2.2.2 Synthesis of N-rGO (Reduced Graphene Oxide)

N-rGO was produced using the streamlined Hummers method (SHM). In the first step, 2 g of fine graphite powder was agitated slowly in a 9:1 (v/v) solution of concentrated H<sub>2</sub>SO<sub>4</sub> and H<sub>3</sub>PO<sub>4</sub> at 50°C for two hours. Slowly, 9 g of solid KMnO<sub>4</sub> was added to the colloid, and the solution was heated at 50°C for 15 hours. After the reaction, a brown colloid was formed, rapidly cooled to 10°C, followed by the dropwise addition of H<sub>2</sub>O<sub>2</sub> solution (5 mL) with continual stirring. The resulting brown colloid was rinsed with distilled water, 30% HCl, and 100% ethanol. The resultant substance is dried in a vacuum oven at 60°C for 12 hours. In the second stage, 150 mg GO was dispersed in 30 mL water using ultrasonication, and then 8 mL of NH<sub>4</sub>OH solution was gently added to the resulting GO suspension. The resultant suspension was then autoclaved at 180°C for 12 hours, separated using a centrifuge at 5,000 rpm, and washed with water, a water-ethanol mixture, and 100% ethanol. Overnight, the final product was dried in a vacuum oven at 60°C. The obtained product was eventually labeled as N-rGO.

**Table 1.** Variations of TSC Composition in NiCo<sub>2</sub>O<sub>4</sub>

Sample Label	Composition of NiCo <sub>2</sub> O <sub>4</sub> : rGO : TSC (mmol : mmol : mmol)
Pristine	1: 1: 0
0.5 mmol TSC	1: 1: 0.5
1 mmol TSC	1: 1: 1
2 mmol TSC	1: 1: 2

## 3. RESULTS AND DISCUSSION

### 3.1 Fabrication of NiCo<sub>2</sub>O<sub>4</sub> Nanoparticles with TSC

The widespread use of NiCo<sub>2</sub>O<sub>4</sub> nanosheets as the primary material for supercapacitor electrodes has been accompanied by low stability. This current study used TSC as a delayed chemical deposition agent on Ni<sup>2+</sup> and Co<sup>2+</sup> in conjunction with NH<sub>4</sub>F as a pseudo-capping agent, a molecule that prevents particle aggregation under hydrothermal conditions (Jiang et al., 2022). Figure 1 depicts a schematic of the synthesis of NiCo<sub>2</sub>O<sub>4</sub> using TSC as a supercapacitor material. At 150°C, Ni<sup>2+</sup> and Co<sup>2+</sup> ions combine with OH<sup>-</sup> ions to generate NiCo precursor crystallites. Additionally, adding OH<sup>-</sup> ions causes Co<sup>2+</sup> ions to precipitate into Co(OH)<sub>2</sub> slowly, generating nascent crystallites

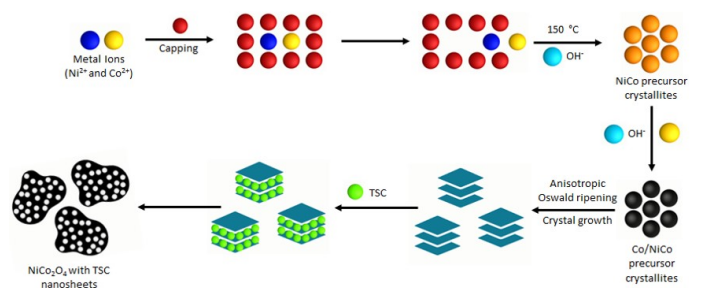


**Figure 1.** Manufacturing Scheme of NiCo<sub>2</sub>O<sub>4</sub> Nanoparticles with Trisodium Citrate (TSC)

distinct from the Co precursors (Lamba et al., 2022). During the process, the pseudo-capping agent (NH<sub>4</sub>F) decomposes, reducing the pH and producing a new crystal precursor called Co/CoNi. In addition, Ostwald's slow anisotropic ripening theory was utilized to determine the transition of Co/NiCo precursors into sheet precursors (Chai et al., 2022). Due to high temperatures, TSC is subsequently ionized as [C<sub>6</sub>H<sub>5</sub>O<sub>7</sub>]<sup>3-</sup> ions, stacked nanosheets capable of reducing hydrogen bonds between layers (Bhardwaj and Jha, 2020). FT-Raman tests on rGO/GO and SEM, FTIR, and XRD analysis on the obtained materials were performed to validate the phase and microstructural properties of the synthesized materials.

### 3.2 SEM Characterization

The objective of the SEM analysis is to observe the morphology of NiCo<sub>2</sub>O<sub>4</sub> with TSC at 1 μm magnification. Figure 2 demonstrates the results of the SEM analysis. According to SEM images in Figure 2.a, NiCo<sub>2</sub>O<sub>4</sub> nanoparticles have a consistent nanowire-like structure. In agreement with the findings of Km et al. (2022), NiCo<sub>2</sub>O<sub>4</sub> nanowires are embedded in a homogenous nanoparticle framework. The advantages of this homogeneous structure can lead to a short ion transport length and a large specific surface area, resulting in the growth of contiguous electrolyte domains. After the addition of TSC to the NiCo<sub>2</sub>O<sub>4</sub> nanoparticles, it was discovered that the addition of 0.5 mmol TSC resulted in a very messy morphological structure (Figure 2.b), the addition of 1 mmol TSC resulted in a neat, more uniform structure that resembled a solid crystal (Figure 2.c), and the addition of 2 mmol TSC resulted in the largest structure. However, the nanoparticles' crystal clarity of 2 mmol TSC sample was poorer than that of 1 mmol TSC sample (Figure 2.d). According to Offor et al. (2021), the denser the morphological structure and the greater the particle size, the higher the TSC addition concentration. Therefore, adding 1 mmol TSC to NiCo<sub>2</sub>O<sub>4</sub> nanoparticles produces the ideal morphological shape, as the structure becomes denser, softer, and more regular.

### 3.3 XRD Characterization

XRD analysis aims to determine whether or not NiCo<sub>2</sub>O<sub>4</sub> nanoparticles contain TSC qualitatively. Figure 3 illustrates



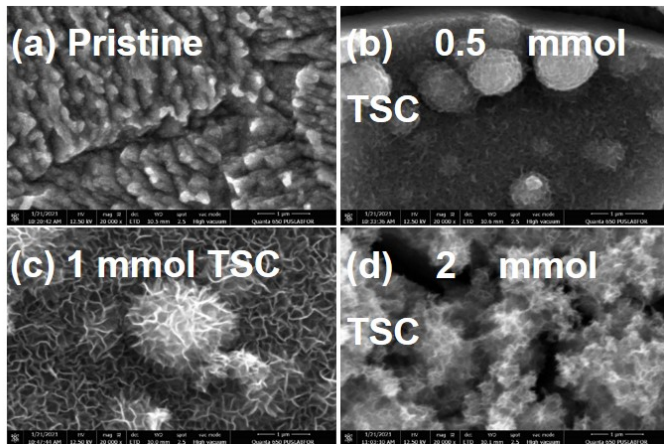


**Figure 2.** SEM Images of (a) Pristine, (b) 0.5 mmol TSC, (c) 1 mmol TSC, and (d) 2 mmol TSC

the XRD patterns. According to Figure 3, almost all of the data do not exhibit differences, or their characteristic peaks had the same pattern, except for the pristine sample, which had a lower peak than the addition of TSC. This suggests that adding TSC does not alter or degrade the crystallinity of the  $\text{NiCo}_2\text{O}_4$  nanoparticles but somewhat improves it. The SEM analysis confirmed that adding 1 mmol of TSC resulted in a consistent, orderly, and smooth arrangement of nanoparticles. The XRD diffraction patterns at  $2\theta$  angles,  $45.04^\circ$  and  $53.34^\circ$  fit the plane of the cubic phase  $\text{NiCo}_2\text{O}_4$  nanorod crystals with values 400 and 511, respectively, as confirmed by JCPDS card no. 20-0781. According to research by Salarizadeh et al. (2020), the angles of  $\text{NiCo}_2\text{O}_4$  nanoparticles at  $2\theta$  are  $44.54^\circ$  and  $59.16^\circ$ . Even though just two significant peaks are evident on the diffractogram, it may be assumed that the identification of TSC on  $\text{NiCo}_2\text{O}_4$  was effective, indicating that it did not disrupt or alter the crystalline structure of  $\text{NiCo}_2\text{O}_4$ . According to Figure 3, the  $\text{NiCo}_2\text{O}_4/\text{rGO}$  composite exhibited no carbon-related distinctive peaks in its XRD pattern. This is owing to the ability of  $\text{NiCo}_2\text{O}_4$  to diminish the strength of rGO diffraction. In addition, FT-Raman spectrum analysis demonstrates the presence of rGO (Du et al., 2016).

### 3.4 Raman Characterization

rGO and GO were analyzed with FT-Raman equipment to determine the nature of the bonding. Figure 4 displays the results of the FT-Raman spectroscopic analysis. According to the investigation results, the distinctive spectra of rGO and GO are very characteristic around  $1360$  (D band) and  $1595$  (G band)  $\text{cm}^{-1}$  for the Raman shift. This shows that rGO and GO molecules contain C=C double bonds. The peak of the Raman G band results from the in-plane motion of  $\text{sp}^2$  carbon, whereas the peak of the Raman D band results from out-of-plane ( $\text{sp}^3$ ) vibrations (Salarizadeh et al., 2020). In contrast, the strength of the rGO peak in the Raman spectrum is greater than that of the GO peak. This is consistent with Aksu et al.

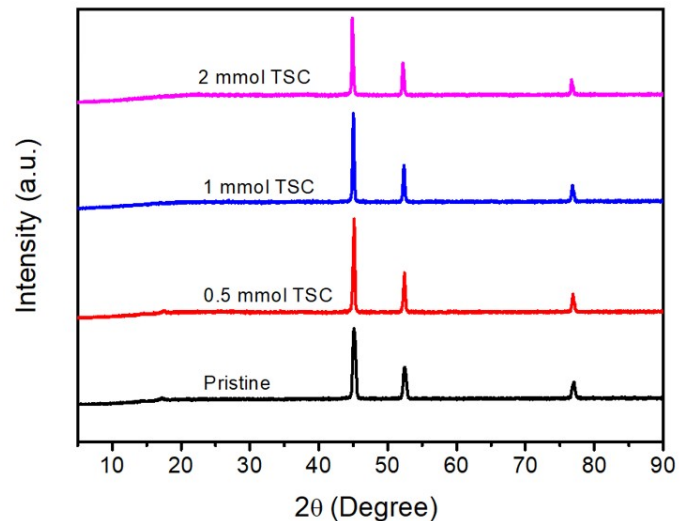


**Figure 3.** XRD Pattern of Pristine (black), 0.5 mmol TSC (red), 1 mmol TSC (blue), and 2 mmol TSC (pink)

(2022), who compared rGO and GO using Raman instruments and revealed C=C bonds with greater peak intensities in rGO. Adding rGO to  $\text{NiCo}_2\text{O}_4$  nanoparticles is intended to improve their electrical conductivity by facilitating charge transfer and promoting uniform material development (Singh et al., 2020). The synergistic impact of  $\text{NiCo}_2\text{O}_4$  sheet and rGO facilitates rapid electronic diffusion, hence enhancing velocity capability and surface activity for charge storage (Jiang et al., 2018). This is also consistent with the findings of Du et al. (2016), who found that rGO addition on  $\text{NiCo}_2\text{O}_4$  of supercapacitors can reach a power conversion efficiency of 6.17%, but without rGO, it is only 5.21%. Without rGO on  $\text{NiCo}_2\text{O}_4$  nanobelts, they tend to congregate and create sarciniform patterns rather than spread out. With the addition of rGO, the  $\text{NiCo}_2\text{O}_4$  nanoparticles dispersed equally across the graphene sheet. In addition, due to the presence of rGO, the composite's efficiency and stability are enhanced.

### 3.5 FTIR Characterization

Functional groups in  $\text{NiCo}_2\text{O}_4$  nanoparticles were identified using FTIR before and after the material synthesis. Figure 5 illustrates the FTIR results of the modified  $\text{NiCo}_2\text{O}_4$  before and after the addition of TSC. Comparing the FTIR spectra before and after the addition of TSC reveals that some vibration spectra shift to longer or shorter wavenumbers while others appear. At wavenumbers of  $1550\text{--}1600\text{ cm}^{-1}$ , it is either a C=C functional group in an aromatic ring or a C=O  $\pi\text{-}\pi$  structure, a bond from rGO (Aman et al., 2022). This was strengthened by pristine,  $\text{NiCo}_2\text{O}_4/\text{rGO}$  nanoparticle, while adding 0.5, 1, and 2 mmol causes a shift, and the peak of the C=C functional group weakens or competes with TSC, which possesses the C=O functional group. A possible cause is the existence of a TSC molecule that degrades rGO, allowing TSC to predominate. A peak confirms this assertion at around  $2300\text{ cm}^{-1}$ ,

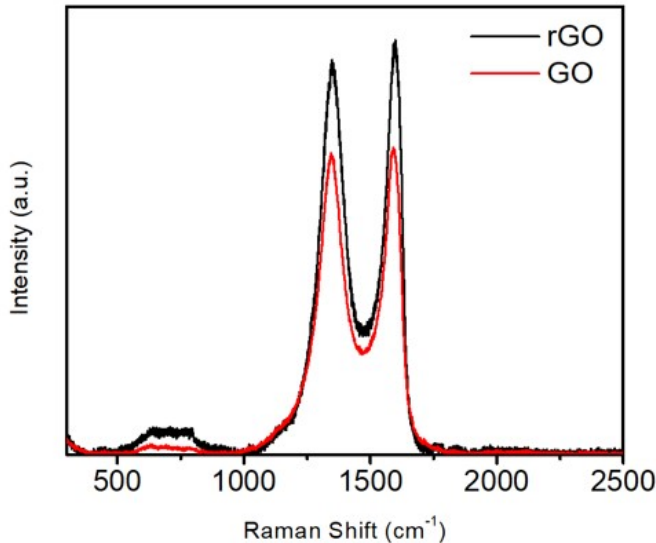


**Figure 4.** FT-Raman Analysis on rGO (black) and GO (red)

corresponding to the OH group in TSC, an alkanolate derivative. More moles of TSC added to  $\text{NiCo}_2\text{O}_4$  nanoparticles will result in sharper peaks. The 2 mmol TSC has the clearest peak IR spectrum compared to the others. At around  $1500\text{ cm}^{-1}$ , a tiny peak corresponds to the Co-O bond in  $\text{NiCo}_2\text{O}_4$  (Aman et al., 2022).

The functional groups on  $\text{NiCo}_2\text{O}_4$  nanoparticles containing rGO as pristine and TSC may be detected using FTIR analysis. Assuming that TSC has been effectively produced on  $\text{NiCo}_2\text{O}_4$  nanoparticles, the results of other characterization experiments with different instruments have also been evaluated. However, additional testing is required to determine the stability of  $\text{NiCo}_2\text{O}_4$  nanoparticles with TSC.

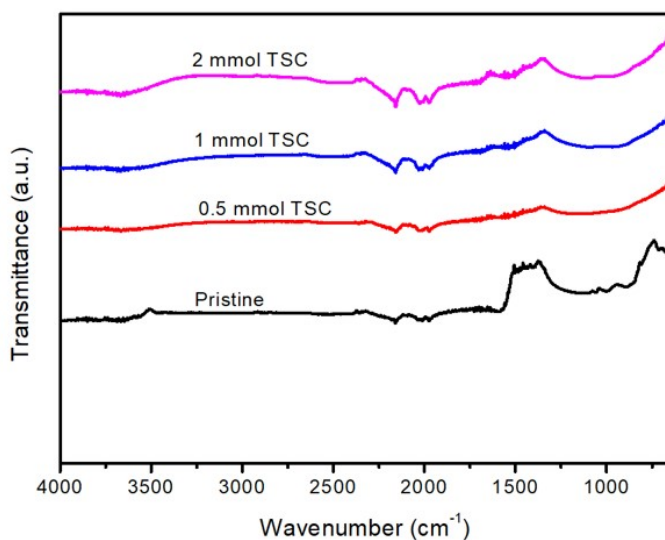


**Figure 5.** FTIR Spectra of Pristine, 0.5 mmol TSC, 1 mmol TSC, and 2 mmol TSC

#### 4. CONCLUSION

The characterization tests conducted using SEM, XRD, FT-Raman, and FTIR indicate that  $\text{NiCo}_2\text{O}_4$  has been successfully synthesized utilizing TSC. At XRD, the angles of  $2\theta$ , namely  $45.04^\circ$  and  $53.34^\circ$ , matched the plane of the cubic phase nanorod crystals of  $\text{NiCo}_2\text{O}_4$  with values of 400 and 511, respectively. In the Raman study, the presence of rGO, which increased the crystallinity of  $\text{NiCo}_2\text{O}_4$  nanoparticles, was confirmed. FTIR analysis determined that the  $1550\text{--}1600\text{ cm}^{-1}$  corresponds to a C=C functional group in an aromatic ring or a C=O  $\pi$ - $\pi$  structure, and the wavenumber of  $2300\text{ cm}^{-1}$  corresponds to the OH group in TSC, which is an alkanolate derivative. SEM analysis determined that  $\text{NiCo}_2\text{O}_4$  nanoparticles with 1 mmol TSC are the best-comparing material for supercapacitor electrodes, as the structure is the most uniform, soft, and tidy. In addition, if the energy is stable, it is possible to stabilize the structure to store energy and process heat. Therefore, further analysis is needed to confirm the stability of the obtained materials.

#### 5. ACKNOWLEDGMENT

The authors would like to thank the Physics Laboratory of Universitas HKBP Nommensen Pematangsiantar and the Physics Laboratory of the National Research and Innovation Agency (BRIN) for providing facilities and instrumental analysis in this research.

#### REFERENCES

- Abdah, M. A. A. M., N. H. N. Azman, S. Kulandaivalu, and Y. Sulaiman (2020). Review of the Use of Transition-metal-oxide and Conducting Polymer-based Fibres for High-performance Supercapacitors. *Materials & Design*, **186**; 108199
- Aksu, Z., C. H. Şahin, and M. Alanyahoğlu (2022). Fabrication of Janus GO/rGO Humidity Actuator by One-step Electrochemical Reduction Route. *Sensors and Actuators B: Chemical*, **354**; 131198
- Aman, S., M. Z. Ansari, M. Abdullah, A. G. Abid, I. Bashir, M. U. Nisa, S. Manzoor, A. M. Shawky, S. Znaidia, and H. M. T. Farid (2022). Facile Synthesis of  $\text{CoCo}_2\text{O}_4/\text{rGO}$  Spinel Nanoarray as a Robust Electrode for Energy Storage Devices. *Inorganic Chemistry Communications*, **146**; 110136
- Bhardwaj, R. and R. Jha (2020). Trisodium Citrate Assisted Morphology Controlled Synthesis of Nickel Sulphide Nanoparticles with Enhanced Cyclic Stability as Carbonaceous Free Electrode Material. *Materials Chemistry and Physics*, **255**; 123581
- Bhat, M. Y., S. Hashmi, M. Khan, D. Choi, and A. Qurashi (2023). Frontiers and Recent Developments on Supercapacitor's Materials, Design, and Applications: Transport and Power System Applications. *Journal of Energy Storage*, **58**; 106104
- Chai, L., Y. Wang, Z. Jia, Z. Liu, S. Zhou, Q. He, H. Du, and G. Wu (2022). Tunable Defects and Interfaces of Hi-

- erarchical Dandelion-like NiCo<sub>2</sub>O<sub>4</sub> via Ostwald Ripening Process for high-efficiency Electromagnetic Wave Absorption. *Chemical Engineering Journal*, **429**; 132547
- Dong, W., L. An, X. Wang, B. Li, B. Chen, W. Tang, C. Li, and G. Wang (2011). Controlled Synthesis and Morphology Evolution of Nickel Sulfide Micro/nanostructure. *Journal of Alloys and Compounds*, **509**(5); 2170–2175
- Du, F., X. Zuo, Q. Yang, B. Yang, G. Li, H. Tang, H. Zhang, M. Wu, and Y. Ma (2016). The Stabilization of NiCo<sub>2</sub>O<sub>4</sub> Nanobelts Used for Catalyzing Triiodides in Dye-sensitized Solar Cells by the Presence of RGO Sheets. *Solar Energy Materials and Solar Cells*, **149**; 9–14
- Faraji, S. and F. N. Ani (2015). The Development Supercapacitor from Activated Carbon by Electroless Plating—a Review. *Renewable and Sustainable Energy Reviews*, **42**; 823–834
- Han, D., P. Xu, X. Jing, J. Wang, P. Yang, Q. Shen, J. Liu, D. Song, Z. Gao, and M. Zhang (2013). Trisodium Citrate Assisted Synthesis of Hierarchical NiO Nanospheres with Improved Supercapacitor Performance. *Journal of Power Sources*, **235**; 45–53
- Jiang, J., Y. Zhang, P. Nie, G. Xu, M. Shi, J. Wang, Y. Wu, R. Fu, H. Dou, and X. Zhang (2018). Progress of Nanostructured Electrode Materials for Supercapacitors. *Advanced Sustainable Systems*, **2**(1); 1700110
- Jiang, M., L. Zhu, Q. Zhao, G. Chen, Z. Wang, J. Zhang, L. Zhang, J. Lei, and T. Duan (2022). Novel Synthesis of NaY-NH<sub>4</sub>F-Bi<sub>2</sub>S<sub>3</sub> Composite for Enhancing Iodine Capture. *Chemical Engineering Journal*, **443**; 136477
- Karimi, F., S. Korkmaz, C. Karaman, O. Karaman, and İ. A. Kariper (2022). Engineering of GO/MWCNT/RuO<sub>2</sub> Ternary Aerogel for High-performance Supercapacitor. *Fuel*, **329**; 125398
- Karthikeyan, S., B. Narenthiran, A. Sivanantham, L. D. Bhatlu, and T. Maridurai (2021). Supercapacitor: Evolution and Review. *Materials Today*, **46**; 3984–3988
- Km, D. K., J. G. Hong, J. Kweon, G. Saeed, K. H. Kim, D. Lee, and M. C. Kang (2022). Spinel NiCo<sub>2</sub>O<sub>4</sub> Nanowires Synthesized on Ni Foam as Innovative Binder-free Supercapacitor Electrodes. *Materials Chemistry and Physics*, **291**; 126718
- Lamba, P., P. Singh, P. Singh, P. Singh, A. Kumar, M. Gupta, and Y. Kumar (2022). Recent Advancements in Supercapacitors Based on Different Electrode Materials: Classifications, Synthesis Methods and Comparative Performance. *Journal of Energy Storage*, **48**; 103871
- Lee, D., K. S. Kim, J. M. Yun, S. Y. Yoon, S. Mathur, H. C. Shin, and K. H. Kim (2019). Synergistic Effects of Dual Nano-type electrode of NiCo-nanowire/NiMn-nanosheet for High-energy Supercapacitors. *Journal of Alloys and Compounds*, **789**; 119–128
- Liu, R., A. Zhou, X. Zhang, J. Mu, H. Che, Y. Wang, T. T. Wang, Z. Zhang, and Z. Kou (2021). Fundamentals, Advances and Challenges of Transition Metal Compounds-based Supercapacitors. *Chemical Engineering Journal*, **412**; 128611
- Manalu, A., K. Tarigan, S. Humaidi, M. Ginting, and I. P. Manalu (2022). Effect of Surface Area on Electrical Properties of NiCo<sub>2</sub>O<sub>4</sub>-reduced Graphene Oxide Nanocomposites for Supercapacitor Electrodes Applications. *Materials Science for Energy Technologies*, **5**; 444–451
- Mehta, S., S. Jha, and H. Liang (2020). Lignocellulose Materials for Supercapacitor and Battery Electrodes: A Review. *Renewable and Sustainable Energy Reviews*, **134**; 110345
- Najib, S. and E. Erdem (2019). Current Progress Achieved in Novel Materials for Supercapacitor Electrodes: Mini Review. *Nanoscale Advances*, **1**(8); 2817–2827
- Nakhodchari, M. M., M. Seifi, and M. T. T. Moghadam (2023). Ternary MnCo<sub>2</sub>O<sub>4</sub>/MWCNT/rGO Nanocomposites as High-performance Supercapacitor Electrode Materials. *Journal of Physics and Chemistry of Solids*, **174**; 111170
- Offor, P., S. Ude, G. Whyte, F. Otung, I. Madiba, A. Bashir, N. Thovhogi, B. Okorie, and F. I. Ezema (2021). Effect of Concentration of Trisodium Citrate Complexing Agent on Spray-synthesized ZnS Thin Films. *Materials Today: Proceedings*, **36**; 133–140
- Paliwal, M. K. and S. K. Meher (2020). Co<sub>3</sub>O<sub>4</sub>/NiCo<sub>2</sub>O<sub>4</sub> Perforated Nanosheets for High Energy Density All Solid State Asymmetric Supercapacitors with Extended Cyclic Stability. *ACS Applied Nano Materials*, **3**(5); 4241–4252
- Ren, H. and C. Huang (2022). Progress in Electrode Modification of Fibrous Supercapacitors. *Journal of Energy Storage*, **56**; 106032
- Saikia, B. K., S. M. Benoy, M. Bora, J. Tamuly, M. Pandey, and D. Bhattacharya (2020). A Brief Review on Supercapacitor Energy Storage Devices and Utilization of Natural Carbon Resources as Their Electrode Materials. *Fuel*, **282**; 118796
- Salarizadeh, P., M. B. Askari, M. Seifi, S. M. Rozati, and S. S. Eisazadeh (2020). Pristine NiCo<sub>2</sub>O<sub>4</sub> Nanorods Loaded rGO Electrode as a Remarkable Electrode Material for Asymmetric Supercapacitors. *Materials Science in Semiconductor Processing*, **114**; 105078
- Shi, W., J. Zhu, D. H. Sim, Y. Y. Tay, Z. Lu, X. Zhang, Y. Sharma, M. Srinivasan, H. Zhang, and H. H. Hng (2011). Achieving High Specific Charge Capacitances in Fe<sub>3</sub>O<sub>4</sub>-reduced Graphene Oxide Nanocomposites. *Journal of Materials Chemistry*, **21**(10); 3422–3427
- Simon, P. and Y. Gogotsi (2020). Perspectives for Electrochemical Capacitors and Related Devices. *Nature Materials*, **19**(11); 1151–1163
- Singh, A., S. K. Ojha, and A. K. Ojha (2020). Facile Synthesis of Porous Nanostructures of NiCo<sub>2</sub>O<sub>4</sub> Grown on rGO Sheet for High Performance Supercapacitors. *Synthetic Metals*, **259**; 116215
- Wang, J., S. P. Feng, Y. Yang, N. Y. Hau, M. Munro, E. Ferreira Yang, and G. Chen (2015). “Thermal Charging” Phenomenon in Electrical Double Layer Capacitors. *Nano Letters*, **15**(9); 5784–5790
- Winter, M. and R. J. Brodd (2004). What are Batteries, Fuel Cells, and Supercapacitors? *Chemical Reviews*, **104**(10); 4245–4270
- Xing, S., Q. Wang, Z. Ma, Y. Wu, and Y. Gao (2012). Con-

Controlled Synthesis of Mesoporous  $\beta$ -Ni(OH)<sub>2</sub> and NiO Nanospheres with Enhanced Electrochemical Performance. *Materials Research Bulletin*, **47**(9); 2120–2125  
Zheng, H., X. Du, Q. Liu, K. Ou, Y. Cao, X. Fang, Q. Fu, and

Y. Sun (2023). Self Healing and Wide Temperature Tolerant Flexible Supercapacitor Based on Ternary-network Organohydrogel Electrolyte. *International Journal of Hydrogen Energy*, **3**(5); 34–39